to 650 nm. The spectrum was recorded at 25 °C with a 1-cm path length cell. The equilibrium constant was determined from changes in the visible spectrum caused by varying the MeIm concentration in solution with a prepared initial concentration of 1.00×10^{-4} M **18** in toluene.

Acknowledgment. This work was supported by financial assistance from the National Institutes of Health and Protos Corp. of Emeryville, CA. High resolution fast atom bombardment mass spectral determinations were performed by the Midwest Center for Mass Spectrometry, a National Science Foundation Regional Instrumentation Facility (Grant No. CHE 862017.7).

Supplementary Material Available: ^1H-^1H and ^1H-^{13}C 2D NMR spectra of **6**, **12**, and **15**, ^1H 1D, ^{13}C 1D, and ^1H-^1H 2D NMR and UV/vis spectra of **VIAH$_2$**, **VIBH$_2$**, and **VICH$_2$**, UV/vis spectra of **17** and **18**, visible spectral changes for the addition of *N*-methylimidazole to a solution of **18** in toluene, a figure showing the sizes of the cavities, and stereoviews of some representative conformers as well as a table of coordinates (.CRD) file and a listing of distances and angles of the most stable conformer (31 pages). Ordering information is given on any current masthead page.

Use of Intermolecular Hydrogen Bonding for the Induction of Liquid Crystallinity in the Side Chain of Polysiloxanes

Uday Kumar, Takashi Kato,† and Jean M. J. Fréchet*

Contribution from the Department of Chemistry, Baker Laboratory, Cornell University, Ithaca, New York 18453-1301. *Received February 26, 1992*

Abstract: A new type of liquid crystalline side chain polysiloxane has been built through self-assembly via intermolecular hydrogen bonding between H-bond donor and acceptor moieties. Poly(methylsiloxanes) and poly(methyl-*co*-dimethylsiloxanes) with side chains containing 4-alkoxybenzoic acid pendant groups attached through aliphatic spacers were synthesized for use as H-bond donor polymers. *trans*-4-[(4-Methoxybenzoyl)oxy]-4′-stilbazole and *trans*-4-ethoxy-4′-stilbazole were prepared as representative mesogenic or nonmesogenic H-bond acceptors, respectively. Formation of the liquid crystalline polymeric complexes occurs by self-assembly of the carboxylic acid group of the polysiloxanes with the stilbazoles through H-bonding as confirmed by spectroscopic techniques. New and extended mesogens result from self-assembly and formation of a single H-bond between the carboxylic acid side chain and the pyridyl group of the stilbazoles. Formation of a side-chain liquid crystalline polymer complex does not require that either or both of the H-bonded fragments display liquid crystallinity. The phase diagrams of a variety of mixtures of the polysiloxanes and the stilbazoles have been established using synchrotron X-ray data, differential scanning calorimetry, and optical microscopy. They show complete miscibility and unusually high thermal stability of the liquid crystals over the whole composition range. X-ray diffraction studies on unoriented samples point to smectic C or smectic A phases for the various complexes. X-ray, DSC, and optical microscopy also show that several of the starting polysiloxanes themselves have smectic C phases with their alkyl chains in an extended conformation. This liquid crystallinity results from dimerization of the benzoic acid moieties.

Introduction

Liquid crystalline polymers have great potential for various functional and high-performance materials.[1,2] For conventional side-chain liquid crystalline polymers, mesogenic units based on homologs of low molecular weight liquid crystals are attached to the polymer backbones as pendant groups through flexible aliphatic spacers using covalent bonding.[3-5] Polymethacrylates, polyacrylates, and polysiloxanes are generally used as the backbones of choice for side-chain liquid crystalline polymers. The most frequently used side-chain mesogens have cyano, nitro, or alkoxy groups as terminal units because these groups induce dipole–dipole intermolecular interactions, which contribute to the overall stability of the mesophase. When these polymers are used for electro-optic devices, the presence of such dipoles is also of great importance in aligning the mesogens in an applied electric field.

In addition to dipole–dipole interactions, various molecular interactions may widen the varieties of liquid crystalline polymers that are available. Our strategy is to utilize H-bonding as the powerful intermolecular interaction ultimately responsible for overall mesomorphicity to create a new class of side-chain liquid crystalline polymers. Hydrogen bonding is one of the key interactions for molecular aggregates in nature. However, intermolecular hydrogen bonding has, in the past, been considered deleterious for thermotropic liquid crystallinity, except for a few systems.[6-9] We have hypothesized that proper control of hydrogen bonding greatly induces the molecular ordering of thermotropic

Scheme I

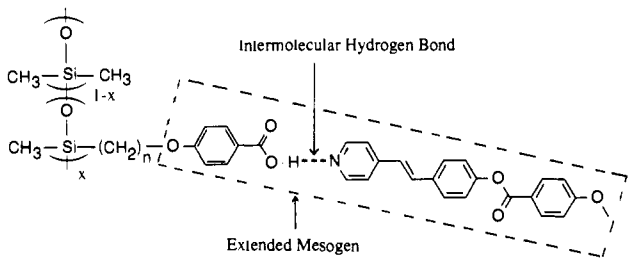

liquid crystals. Our initial approach[10] involved a 4-oxybenzoic acid moiety (capable of H-bonding interactions) that was introduced as a pendant group on a polyacrylate backbone. Subsequent complex formation between this polymer and a stilbazole moiety

† Present address: University of Tokyo, Institute of Industrial Science, Tokyo 106, Japan.

(1) Ciferri, A., Krigbaum, W. R., Meyer, R. B., Eds. *Polymer Liquid Crystals*; Academic: New York, 1982.
(2) Chapoy, L. L., Ed. *Recent Advances in Liquid Crystalline Polymers*; Elsevier: London, 1985.
(3) Ringsdorf, H.; Schneller, A. *Br. Polym. J.* **1981**, *13*, 430.
(4) Finkelmann, H.; Rehage, G. *Adv. Polym. Sci.* **1984**, *60/61*, 99.
(5) Shibaev, V. P.; Plate, N. A. *Adv. Polym. Sci.* **1984**, *60/61*, 173.
(6) Aharoni, S. M. *Macromolecules* **1988**, *21*, 1941.
(7) Jeffrey, G. A. *Acc. Chem. Res.* **1986**, *19*, 168.
(8) Bennett, G. M.; Jones, B. *J. Chem. Soc.* **1939**, 420.
(9) Gray, G. W.; Jones, B. *J. Chem. Soc.* **1953**, 4179.
(10) Kato, T.; Fréchet, J. M. J. *Macromolecules* **1989**, *22*, 3818; **1990**, *23*, 360.

0002-7863/92/1514-6630$03.00/0

Scheme II

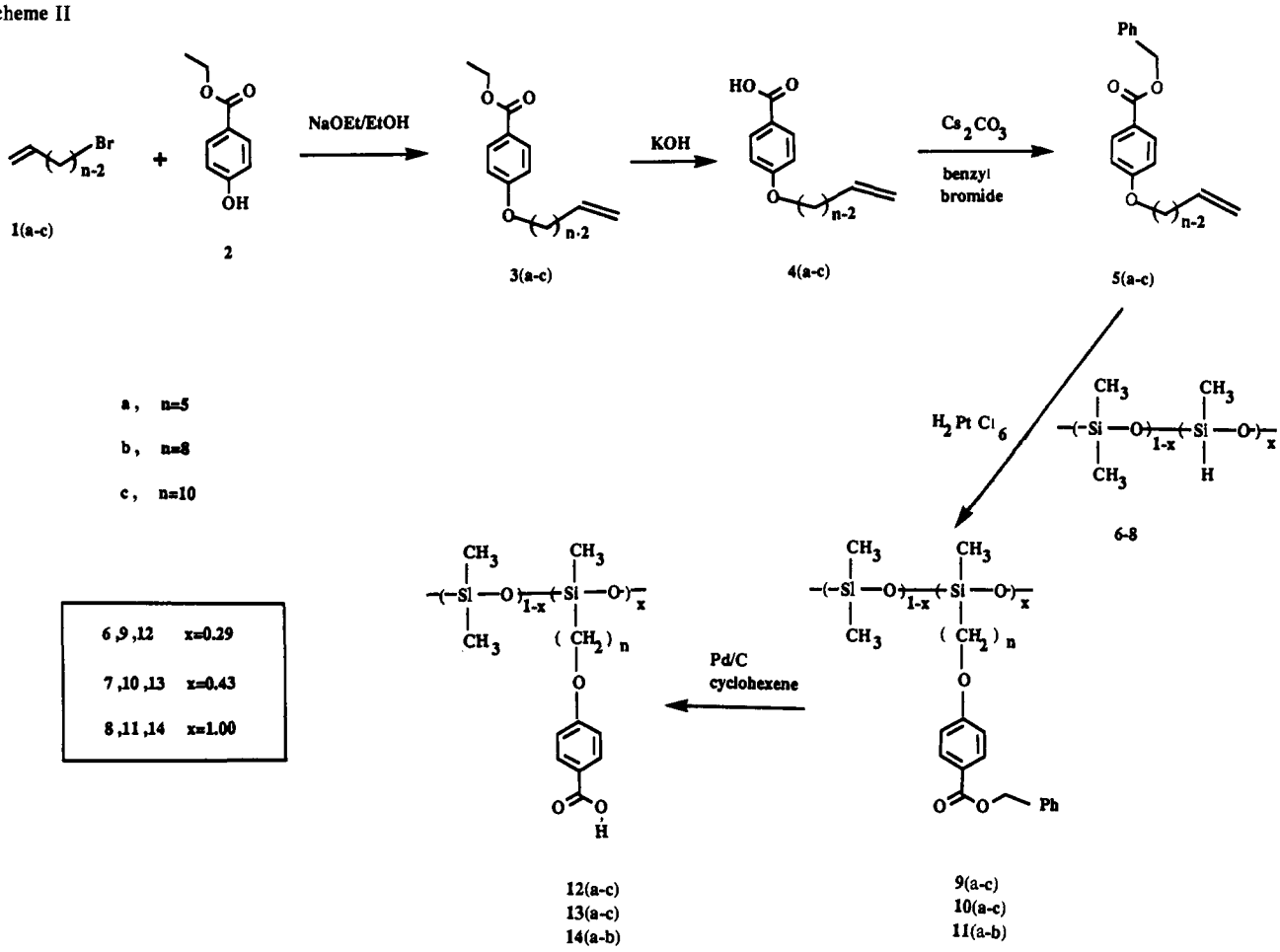

via a self-assembly process resulted in the formation of an extended mesogen which strongly stabilized the mesophase. The novel mesogen was formed through intermolecular hydrogen bonding between the benzoic acid unit and the 4-stilbazole. In this case, the single hydrogen bond between the H-bond donor and the acceptor increased the length to diameter ratio of the H-bonded complex to afford a highly thermally stable product. This approach has also been used successfully in building self-assembling liquid crystalline complexes between different low molecular weight compounds.[11,12] For example, it was found that nonmesogenic compounds can function as two-pronged core units in the formation of twin mesogenic complexes through similar selective H-bonded interactions.

We have considered it especially important to explore the use of such hydrogen bonding between the side chains of polymers and low molecular weight compounds (Scheme I). A thorough understanding of the nature of this type of self-assembled complexes based on polymers would guide us in the introduction of additional functional molecules into the liquid crystalline polymer matrix through H-bonding, which could result in a novel type of functional polymeric materials.

In the present study, polysiloxanes containing a benzoic acid moiety as part of their side chain have been synthesized and found to possess unusual liquid crystalline properties. Their liquid crystallinity results from the formation of H-bonded dimeric structures analogous to those reported by Gray[9] for low molecular weight 4-alkoxybenzoic acids. This family of functionalized polysiloxanes was selected for use as the H-bond donor in complexation to suitable acceptors in view of the well-documented and unique thermotropic properties[13-17] of more classical types of side-chain liquid crystalline polysiloxanes. Mesogenic and nonmesogenic *trans*-4-stilbazole derivatives have been selected as the H-bond acceptor due to the high ΔH values for the formation of H-bonded complexes between carboxylic acids and pyridine.[18] The effect of the hydrogen bonding on the mesomorphic properties has been examined for the various complexes between polysiloxanes and stilbazoles and is reported below.

Results and Discussion

Preparation of the Side Chain (4-Alkoxybenzoic Acid) Terminated Polysiloxanes 12a–c, 13a–c, and 14a,b. Polysiloxanes **12a–c**, **13a–c**, and **14a,b** containing 4-alkoxybenzoic acid terminated pendant groups were synthesized for the first time as shown in Scheme II. Substituents are generally introduced in the side chain of polysiloxanes by a hydrosilylation reaction involving poly(methylhydrosiloxane) or poly(methylhydrosiloxane-*co*-dimethylsiloxane) and an alkene in the presence of hydrogen hexachloroplatinate as the catalyst.[13,14] The synthetic scheme used in this preparation takes into account the fact that hydrosilylation reactions do not proceed quantitatively in the presence of functionalities containing active hydrogens.

The starting materials chosen for the preparation of the side chains were alkenyl halides **1a–c** containing 5, 8, and 10 methylenes, respectively, and ethyl 4-hydroxybenzoate **2**. Benzyl

(11) Kato, T.; Frēchet, J. M. J. *J. Am. Chem. Soc.* **1989**, *111*, 8533. Frēchet, J. M. J.; Kato, T. US Patent 5,037,574, 1991.
(12) Kato, T.; Fujishima, A.; Frēchet, J. M. J. *Chem. Lett.* **1990**, 919. Kato, T.; Wilson, P. G.; Fujishima, A.; Frēchet, J. M. J. *Chem. Lett.* **1990**, 2003. Kato, T.; Adachi, H.; Fujishima, A.; Frēchet, J. M. J. *Chem. Lett.* **1992**, 265.
(13) Finkelmann, H.; Rehage, G. *Makromol. Chem. Rapid Commun.* **1980**, *1*, 31.
(14) Ringsdorf, H.; Schneller, A. *Makromol. Chem. Rapid Commun.* **1982**, *3*, 557.
(15) Harn, B.; Percec, V. *Macromolecules* **1987**, *20*, 2961.
(16) Gray, G. W.; Lacey, D.; Nestor, G.; White, M. S. *Makromol. Chem.* **1987**, *188*, 2759.
(17) Coles, H. *Faraday Discuss. Chem. Soc.* **1985**, *79*, 201.
(18) Odinokov, S. E.; Mashkovsky, A. A.; Glazunov, V. P.; logansen, A. V.; Rassadin, B. V. *Spectrochim. Acta* **1976**, *32A*, 1355.

Table I. Determination of the Degree of Substitution of Polysiloxanes **6–8**, **12a–c**, **13a–c**, and **14a,b** by ^{1}H NMR Spectroscopy[a]

polysiloxane	number of methylene spacer	x	$1-x$
6		0.29	0.71
12a	5	0.30	0.70
13a	8	0.30	0.70
14a	10	0.26	0.74
7		0.43	0.57
12b	5	0.44	0.56
13b	8	0.44	0.56
14b	10	0.40	0.60
8		1.00	0
12c	5	0.96	0.04
13c	8	0.95	0.05

[a] DMSO-d_6 was used as solvent for polysiloxanes **12a–c**, **13a–c**, and **14a,b**. $CDCl_3$ was used as solvent for polysiloxanes **6–8**.

esters **5a–c** were prepared by alkylation of ethyl 4-hydroxybenzoate with ω-alkenyl halides **1a–c**, followed by hydrolysis and re-esterification of the resulting 4-(ω-alkenyloxy)benzoic acids **4a–c** with benzyl bromide. This reaction is a modification of the known method of esterification involving anhydrous cesium salts of the carboxylic acids and alkyl halides in polar aprotic solvents.[19,20] Hydrosilylation reactions of polysiloxanes **6–8** and benzyl esters **5a–c** carried out in the next step proceeded quantitatively in the presence of a 10% excess of the alkene. This excess was removed from the substituted polysiloxane after reaction through flash chromatography using dichloromethane/hexane (2:1) to remove the alkene from the strongly retained polymer and then eluting the substituted polysiloxane with THF. Finally, hydrogenolysis of the benzoate esters of **9a–c**, **10a–c**, and **11a,b** was carried out using 10% Pd/C and cyclohexene as the hydrogen donor. Eight different polymers having structures **12a–c**, **13a–c**, and **14a,b** were prepared by this procedure. While the starting polysiloxane and all intermediate products including **9–11** were oily materials, hydrogenolysis afforded solid polymers with relatively high melting points due to the formation of dimeric structures between pendant side-chain benzoic acid moieties via hydrogen bonding.[9]

^{1}H and ^{13}C NMR spectra of polymer **14a** obtained in DMSO-d_6 solution at 67 °C confirm the structure of the polymer. The signal corresponding to the carboxylic acid proton is seen as a broad band at 3.15 ppm. This assignment is based on the spectrum of benzoic acid in DMSO-d_6 at 67 °C. In addition, the single carbonyl peak seen at 166.5 ppm in the ^{13}C NMR spectrum and the absence of benzylic protons near 5.3 ppm in the ^{1}H NMR spectrum indicate that deprotection of the benzyl ester proceeded quantitatively.

^{1}H NMR spectroscopy was also used to determine the degree of substitution of the starting polymers **6–8** and the final products **12–14**. For polysiloxanes **6–8**, the ratios of SiH to $SiCH_3$ proton peaks were used to determine the copolymer composition. In the case of **6** and **7**, peak areas for all of the methyl groups present in the polymer were used in the determination of the copolymer composition, as the contribution of the trimethylsilyl end groups to the total methyl group content in the polymer is quite small. The ratio of CH_2O to $SiCH_3$ proton peaks at 4.02 and 0.01 ppm, respectively, was used to ascertain the composition of the carboxy-ended polysiloxanes **12a–c**, **13a–c**, and **14a,b**. As can be seen in Table I, the degrees of functionalization of the starting polysiloxanes **6–8** and of the final products **12a–c**, **13a–c**, and **14a,b** remain essentially constant. Therefore the nominal values as determined for the starting polysiloxanes **6–8** will be used in the subsequent discussion and tables.

The molecular weights of the carboxy-ended polysiloxanes **12a–c**, **13a–c**, and **14a,b** determined by gel permeation chromatography (GPC, polystyrene calibration) in combination with viscometry with universal calibration are shown in Table II. The

Table II. Molecular Weights of the Carboxy-Ended Side-Chain Polysiloxanes **12–14**, as Determined by Viscometry with Universal Calibration or by Gel Permeation Chromatography[a]

	viscometry			GPC		
polymer	M_w	M_n	M_w/M_n	M_w	M_n	M_w/M_n
12a	11700	7200	1.6	8700	5600	1.5
12b	11500	7600	1.5	11400	7200	1.6
12c	13800	8800	1.6	14800	8800	1.7
13a	6000	4300	1.4	6300	5000	1.3
13b	7000	4700	1.5	7900	6000	1.3
13c	6700	5300	1.2	7600	6200	1.2
14a	12400	8300	1.5	12400	8800	1.4
14b	12500	8300	1.5	12400	8500	1.5

[a] Values given for polystyrene-calibrated column set.

Table III. Thermal[a,b] Properties of 4-Alkoxybenzoic Acid Terminated Side-Chain Polysiloxanes **12a–c**, **13a–c**, and **14a,b**

polysiloxane	T_g, °C	T_{soft},[d] °C	T_m, °C	$T_{S\rightarrow I}$, °C	ΔH, J/g
12a	31[e]	95		108	12.1
13a	58[e]	125		134	15.9
14a[c]			221		43.8[f]
12b	−7	81		111	8.5
13b	10	79		133	24.0
14b			174	182	27.6
12c	−15	84		108	10.6
13c	−20	89		125	16.5

[a] T_g, glass transition temperature; T_m, melting transition temperature; $T_{S\rightarrow I}$, smectic–isotropic transition temperature. [b] ΔH, enthalpy change for S → I transition in J/g of polysiloxane. [c] Nonmesogenic. [d] T_{soft}, softening temperature, detected by optical microscopy. [e] T_g detectable only during first run. [f] ΔH reported here is for K → I transition.

weight-average molecular weights vary between 6000 and 14000, reflecting the disparity of the starting materials. The low polydispersities measured by GPC may well reflect a process of fractionation occurring during the chromatographic clean-up of the functionalized polymers.

Liquid Crystalline Properties of the Side Chain (*p*-Alkoxybenzoic Acid) Terminated Polysiloxanes 12a–c, 13a–c, and 14a,b. Polysiloxanes **12a–c**, **13a–c**, and **14a,b** were synthesized to be later used as H-bonding donors for the preparation of polymeric hydrogen-bonded complexes. However, we found that these polysiloxanes containing a benzoic acid moiety as a side-chain substituent exhibit thermotropic mesophases. Gray[9] has shown that a number of benzoic acid derivatives exhibit liquid crystallinity due to the formation of H-bonded dimers, but this finding has not been extended to polymer systems until recently. Blumstein and co-workers have studied[21] the properties and structures of poly(*p*-(acryloyloxy)benzoic acid) and poly(*p*-(methacryloyloxy)benzoic acid). No fluid mesomorphic states could be obtained with these polymers upon heating due to the formation of highly cross-linked ordered structures through intermolecular dimerization involving H-bonds. More recently, we observed[10] that a polyacrylate structure such as **15**, containing a pendant 4-oxybenzoic acid unit with a hexamethylene spacer, exhibits a narrow nematic liquid crystalline phase from 140 to 155 °C. In this instance, the introduction of flexibility between the rigid aromatic component used to form the mesogen and the polymer main chain is key to the observation of liquid crystallinity.

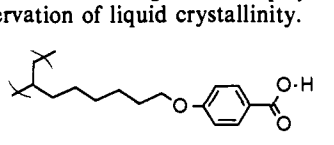

15

The thermal properties of once-annealed samples of polysiloxanes **12a–c**, **13a–c**, and **14a,b** are given in Table III. Once-annealed samples were prepared by cooling from the iso-

(19) Wang, S. S.; Gisin, B. F.; Winter, D. P.; Makofske, R.; Kulesha, I. D.; Tzougraki, C.; Mienhofer, J. *J. Org. Chem.* **1977**, *42*, 1286.
(20) Pfeffer, P. E.; Silbert, L. S. *J. Org. Chem.* **1976**, *41*, 1373.
(21) Blumstein, A.; Clough, S. G.; Patel, L.; Blumstein, R. B.; Hsu, E. C. *Macromolecules* **1976**, *9*, 243.

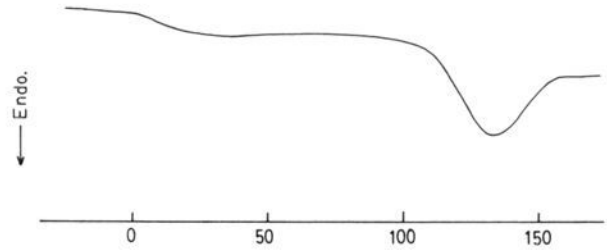

Figure 1. DSC thermogram of polysiloxane **13b**.

Table IV. OH Stretching Frequencies of the COOH Group in Carboxy-Ended Polysiloxanes **12a** and **13a,b** and Its Binary Blends with Stilbazole **16** or **17**

polymer blend	mol % COOH	frequency, cm^{-1}		
12a	100	2570 (m)	2670 (m)	2970 (s)
13a	100	2560 (m)	2675 (m)	2960 (s)
13b	100	2550 (m)	2670 (m)	2930 (s)
13c	100	2540 (m)	2680 (m)	2925 (s)
[12a/16]	50	1940 (m)	2550 (m)	2650 (w)
[13a/16]	50	1940 (m)	2570 (m)	2650 (w)
[13b/16]	50	1920 (m)	2500 (m)	2670 (w)
[12a/17]	50	1975 (m)	2520 (m)	
[13a/17]	50	1950 (m)	2500 (m)	
[13b/17]	50	1960 (m)	2480 (m)	

tropic states. The transition temperatures were determined by DSC and polarized microscopy. Seven of the eight polymers exhibit liquid crystalline behavior due to dimerization of the alkoxybenzoic acid unit. The mesophase is identified as a smectic phase on the basis of visual observation and X-ray diffraction measurements. Figure 1 shows the heating run of the DSC thermogram for the once-annealed sample of polymer **13b**, which is representative for the polysiloxanes **12a–c** and **13b,c**. The glass transition is observed near 10 °C, and the endothermic peak corresponding to the isotropization is seen at 133 °C. The broadness of the smectic to isotropic transition is likely due to the polydisperse nature of the copolymers. Although there is no melting endotherm in the DSC thermogram, the sample shows no fluidity below 79 °C as seen by optical microscopy. Even annealing polymer **13b** at 85 °C for 60 min followed by cooling to below its T_g at 0.5 °C/min does not induce any crystallinity, with the sample remaining in the smectic state throughout. X-ray evidence presented below also confirms that the sample has no crystallinity above its glass transition temperature. Polysiloxane **13b** is smectic above its glass transition temperature, but its fluidity is restricted due to intermolecular dimerization of the pendant oxybenzoic acid unit, resulting in highly cross-linked structures. Upon heating above T_g, the sample shows a fluid mesomorphic state and birefringency due to the dynamic nature of the hydrogen bonds only when a certain temperature listed as T_{soft} in Table III is reached. The values of T_{soft} do not change after several heating and cooling runs. DSC measurements on polysiloxanes **12a** and **13a** show a glass transition only in the first run, a behavior that cannot be explained at this time.

IR frequencies for the carboxy-ended polysiloxanes resemble those of benzoic acid[22] (Table IV). The IR spectra of polysiloxanes **12a** and **13a–c** are dominated by the characteristic bands resulting from self-association of the side-chain carboxylic acid dimer. The OH stretching frequency of the dimer is seen as a broad band at about 3000 cm^{-1} overlapping the strong CH stretching modes. "Satellite" bands of medium intensity, around 2550 and 2650 cm^{-1} (Table IV) superimposed upon the broad fundamental profile,[22] are also observed in the IR spectra of polysiloxanes.

The X-ray diffraction data of nonoriented samples of carboxy-ended polysiloxanes are given in Table V. The diffraction

Table V. X-ray Diffraction Pattern of Some Carboxy-Ended Side-Chain Polysiloxanes Taken at Different Temperatures

polymer	temp,[a] °C	layer spacing[b] *d*, Å
12a	75	29.7 (s), 7.9 (d)
	103	29.0 (s), 7.9 (d)
13a	130	26.9 (s), 13.8 (w), 8.0 (d)
13b	60	60.0 (m), 33.2 (s), 29.0 (m)
		16.6 (w), 11.0 (w), 7.8 (d)
	125	32.0 (s), 15.4 (w), 10.6 (w), 7.8 (d)
	125[c]	33.2 (s), 15.8 (w), 10.8 (w), 8.0 (d)
	60[c]	56.0 (m), 33.2 (s), 29.0 (m)
		16.4 (w), 11.0 (w), 7.6 (d)
13c	40	36.4 (s), 18.4 (m), 12.1 (m), 7.6 (d)
	80	36.4 (s), 18.1 (m), 12.1 (w), 7.6 (d)
	90	36.1 (s), 18.2 (m), 11.6 (w), 7.6 (d)
	120	35.4 (s), 17.6 (m), 11.8 (m), 7.8 (d)

[a] All temperatures reported are for the heating run. s, m, w, and d are strong, medium, weak, and diffuse reflections, respectively. [b] A diffuse ring centered around 4.5 Å is seen in all films. [c] Sample heated to isotropization and cooled to 125 and 60 °C, respectively.

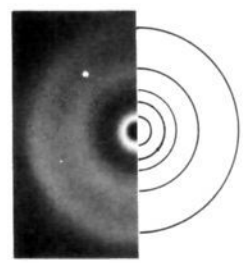

Figure 2. X-ray diffraction of **13b** at 125 °C (heating run).

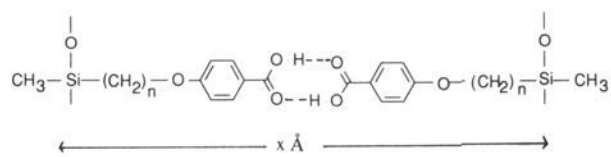

A, n = 5 x = 31
B, n = 8 x = 39
C, n = 10 x = 44

Figure 3. Molecular lengths of low molecular weight analogs of carboxy-ended side-chain polysiloxanes **12–14**.

pattern of **13b** at 125 °C (heating run) is shown in Figure 2. The diffraction pattern can be divided into inner and outer rings occurring at small and large diffraction angles, respectively. The inner rings are indicative of layer spacings and the outer rings of intermolecular spacings within a layer. As seen in Table V, the Bragg reflections for **13b** show the polymer to have no crystallinity between the glass transition temperature, T_g, and the softening temperature, T_{soft}. On heating the polysiloxane **13b** to 125 °C, five reflections appear at 4.6, 7.8, 10.6, 15.4, and 32.0 Å, respectively. The absence of sharp outer rings (Table V and diffraction photograph in Figure 2) indicates that higher order smectics such as S_B, S_G, S_H, and S_E are not present.[23,24] The broad halo centered at 4.6 Å indicates that the lateral packing within the smectic layer is disordered. The value of 4.6 Å roughly corresponds to the width of a single mesogen. The presence of a broad diffuse outer ring extending from 5.2 to 4.2 Å (Figure 2) suggests an S_A or S_C phase and rules out a smectic F phase for **13b**,[25,26] as the latter tends to give an outer ring with an

(22) (a) Bratoz, S.; Hadzi, D.; Sheppard, N. *Spectrochim. Acta* **1956**, *8*, 249. (b) Lee, J. Y.; Painter, P. C.; Coleman, M. M. *Macromolecules* **1980**, *21*, 346.

(23) Krigbaum, W. R.; Watanabe, J.; Ishikawa, T. *Macromolecules* **1983**, *16*, 1271.

(24) Taylor, T. R.; Fergason, J. L.; Arora, S. L. *Phys. Rev. Lett.* **1970**, *24*, 359.

(25) Benattar, J. J.; Doucet, J.; Lambert, M.; Levulet, A. M. *Phys. Rev. A* **1979**, *20*, 2505.

(26) Benattar, J. J.; Moussa, F.; Lambert, M. *J. Phys. Lett.* **1981**, *42*, L67.

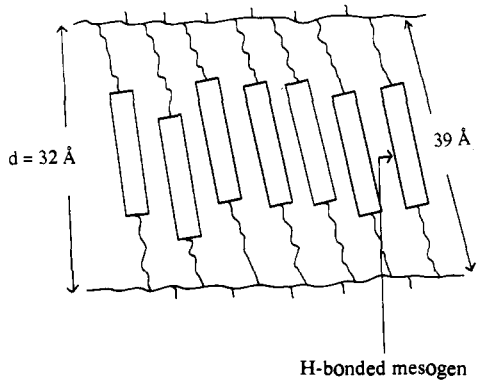

Figure 4. Schematic of the smectic C layer of polysiloxane **13b** at 125 °C as determined by X-ray diffraction. d = layer spacing in Å.

Table VI. Tilt Angle of Some Representative Carboxy-Ended Polysiloxanes Measured by X-ray Diffraction

polymer	temp, °C	tilt angle,[a] deg
12a	75	17
	103	21
13a	130	30
13b	125	35
	125[b]	32
13c	40	34
	80	34
	90	35
	120	36

[a] Error in tilt angle is ±5°, due to error in molecular modeling and measurement of layer spacing by X-ray diffraction.

intensity spread of only 0.2–0.3 Å.[25] The presence of another broad halo at 7.8 Å probably indicates microphase separation between the mesogenic oxybenzoic acid dimer and nonmesogenic dimethylsiloxane backbone moieties.

The strong inner ring at 32.0 Å corresponds to the thickness or width of the smectic layer, while the weak diffractions at 15.4 and 10.6 Å are due the second- and third-order reflections of the smectic layer. Molecular modeling (using standard bond lengths and bond angles) of the low molecular weight analog of **13b**, with the methylene units in their fully extended conformation, gives a mesogenic length of 39 Å (Figure 3B). The layer spacing of 32 Å being substantially less than the mesogenic length of 39 Å points to an S_C phase as illustrated in Figure 4. The repeat unit shown in Figure 4 corresponds to the polymeric analog (**13b**) of the H-bonded dimer shown in Figure 3B. The presence of an S_C phase for **13b** is confirmed by optical microscopy with a characteristic *schlieren* pattern and no focal conic texture. Cooling **13b** to 60 °C (below its T_{soft}) gives another smectic layer at 56.0 Å, with its second-order reflection appearing at 29.0 Å (Table V). Therefore, two kinds of smectic C phases S_{C1} and S_{C2}, or domains with a layer spacing of 33 and 56 Å, coexist on cooling the sample to below its softening temperature. The coexistence of two types of smectic layers has been observed previously in some polyacrylates.[27] Polysiloxanes **12a–c** and **13a–c** show diffraction patterns similar to that of **13b** in the fluid state. For a fixed copolymer composition, the layer spacing increases linearly in the series **13a** → **13c**, indicating that the alkyl chains are in an extended conformation. Tilt angles[28] of some representative polysiloxanes are shown in Table VI. Tilt angles were calculated from the expression $d = d_0 \cos \theta$, where d represents the smectic layer spacing and d_0 is the mesogenic length obtained from molecular modeling with the methylene units in their fully extended conformation (Figure 3). The constancy of the tilt angle for **13a–c** indicates that, for a given copolymer composition, the structure

(27) Kostromin, S. G.; Sinitzyn, V. V.; Talroze, R. V.; Shibaev, T. V. *Makromol. Chem. Rapid Commun.* **1982**, *3*, 809.
(28) Martinot-Lagarde, P.; Duke, R.; Durand, G. *Mol. Cryst. Liq. Cryst.* **1981**, *75*, 249.

Scheme III

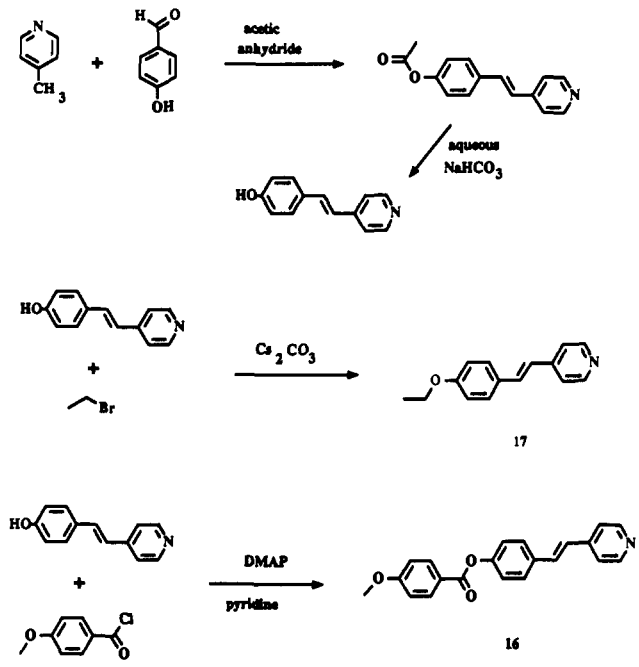

of the repeat unit of the smectic phase is the same regardless of alkyl chain length.

It is likely that the dimethylsiloxane portions of the polymer chain contribute to the formation of the amorphous phase, as can be seen in the lowering of T_g values for polymers **12a–c** and **13a–c** as the number of methylene spacers increases (Table III). Decoupling of the motions of the main chain and of the side chain is facilitated by increased spacer length, and the glass transition temperatures, T_g, of the polysiloxanes tend to approach that of poly(dimethylsiloxane) as the spacer length increases.

Although the molecular weights of the various copolymers **12a–c**, **13a–c**, and **14a,b** vary (Table II), the transition temperatures given in Table III reflect the effect of the dilution of the mesogenic units by the nonmesogenic dimethylsiloxane moieties. For a given length of methylene spacer, both T_g and the temperature of smectic to isotropic (S → I) transition decrease on dilution of the mesogenic groups with nonmesogenic dimethylsiloxane groups. The decrease in S → I transition temperature is particularly significant when comparing a homopolymer such as **14b** with the corresponding copolymer **13b** due to the drastic decrease in the number of hydrogen bonds which contribute to the crystallinity of the polysiloxane.

The liquid crystallinity of polymers **12a–c**, **13a–c**, and **14a,b** is induced by the formation of the H-bonded dimeric structures[9] between the 4-(alkyloxy)benzoic acid units of the polymer side chains, a process which amounts to cross-linking of the polymers. It is interesting to note that, despite the occurrence of this cross-linking, the polymers remain soluble in appropriate solvents such as THF or pyridine. This type of *reversible cross-linking* is of additional interest for practical use in devices due to the ease with which it can be affected by thermal events or the addition of competing H-bond acceptors.

Complexation of Side Chain (4-Alkoxybenzoic Acid) Terminated Polysiloxanes 12a–c, 13a–c, and 14a,b with Mesogenic *trans*-4-[(4-Methoxybenzoyl)oxy]-4′-stilbazole (16). In order to explore the effect of the formation of H-bonds between dissimilar species on their mesomorphic properties, polymers **12a–c**, **13a–c**, and **14a–c** were complexed with *trans*-4-[(4-methoxybenzoyl)oxy]-4′-stilbazole (**16**). Stabilization of the resulting complexes (Scheme I) by the lateral dipoles of the carbonyl and pyridyl groups may give rise to tilted smectic phases. The technique used in the formation of these complexes involves the dissolution of both components in pyridine, which causes the breaking of existing H-bonds within the polymer, followed by the slow evaporation

Table VII. Transition Temperatures[a] of 1:1 Complexes[b] of Polysiloxanes **12a–c**, **13a–c**, and **14a,b** and *trans*-4-[(4-Methoxybenzoyl)oxy]-4′-stilbazole (**16**)[c] (Prepared from Pyridine Solution)

1:1 complex	T_g, °C	$T_{K\rightarrow S}$, °C	$T_{S\rightarrow I}$, °C	ΔH_1,[d] J/g	ΔH_2,[e] J/g
[**12a**/**16**]	21	82	227	4.1	9.6
[**13a**/**16**]	7	126	229	9.7	11.0
[**14a**/**16**]	15	134	247	9.8	7.1
[**12b**/**16**]	12	56	230	3.0	9.0
[**13b**/**16**]	16	63	239		13.7
[**14b**/**16**]	25	134	252	8.6	10.8
[**12c**/**16**]	8	49	239	1.0	10.3
[**13c**/**16**]	16	64	238	1.5	9.0

[a] T_g, glass transition temperature; $T_{K\rightarrow S}$, crystalline to smectic transition temperature; $T_{S\rightarrow I}$, smectic–isotropic transition temperature. [b] Equimolar amounts of the COOH group of the polysiloxane and the stilbazole were used. [c] Transition temperatures: $T_{K\rightarrow N}$, 168 °C; $T_{N\rightarrow I}$, 216 °C. [d] ΔH_1, enthalpy change for K → S transition in J/g of polymer blend. [e] ΔH_2, enthalpy change for S → I transition in J/g of polymer blend.

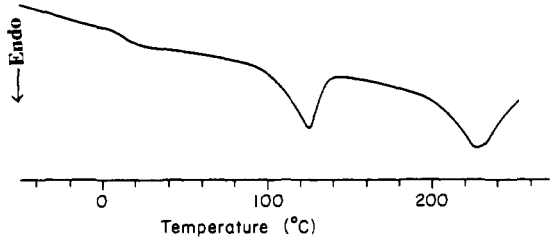

Figure 5. DSC thermogram of the complex between polysiloxane **13a** and stilbazole **16**: (A) heating run of the complex annealed to 220 °C; (B) cooling run.

of the pyridine,[10,29] resulting in the self-assembly of the final complexes.

Stilbazole **16**, which exhibits a nematic phase from 168 to 216 °C,[30] was prepared from 4-methoxybenzoyl chloride and *trans*-4-hydroxy-4′-stilbazole, itself obtained by a modification of the procedure of Chiang and Hartung,[31] as shown in Scheme III.

Table VII shows the transition temperatures and the corresponding enthalpy changes for the various 1:1 complexes between all eight polymers and stilbazole **16**. An equimolar amount of the carboxy group of the polymer and of the stilbazole is used in the formation of each 1:1 complex from pyridine solution. In the following discussion, a 1:1 complex between, for example, polymer **12a** and stilbazole **16** will be identified by the notation [**12a**/**16**]. DSC transitions (Table VII) for [**12a**/**16**] and [**13a**/**16**] were recorded after heating to 220 °C and cooling below T_g. The thermal properties of complexes [**14a**/**16**] through [**13c**/**16**] given in Table VII were obtained for samples that were heated to 200 °C and then cooled to below their T_g. It is important to emphasize that the transition temperatures of the complexes based on polysiloxanes **12a–c**, **13a–c** and **14a,b** and stilbazole **16** are dependent on their thermal histories. The maximum temperatures of the endothermic peaks at melting and isotropization, taken as transition temperatures, were used for Table VII. It is seen clearly that the mesophases of the various complexes are stabilized and exist at temperatures far higher than those of either of their individual components. For example, complex [**13b**/**16**] shows a smectic phase between 63 and 239 °C during the heating run, whereas the individual components **13b** and **16** become isotropic at 133 and 216 °C, respectively. We attribute this stabilization of the mesophase to the formation of the H-bonded mesogen between the pendant benzoic acid moiety and the stilbazole as shown in Scheme I. This new and extended mesogen is quite unique because, as will be demonstrated below, it is a single

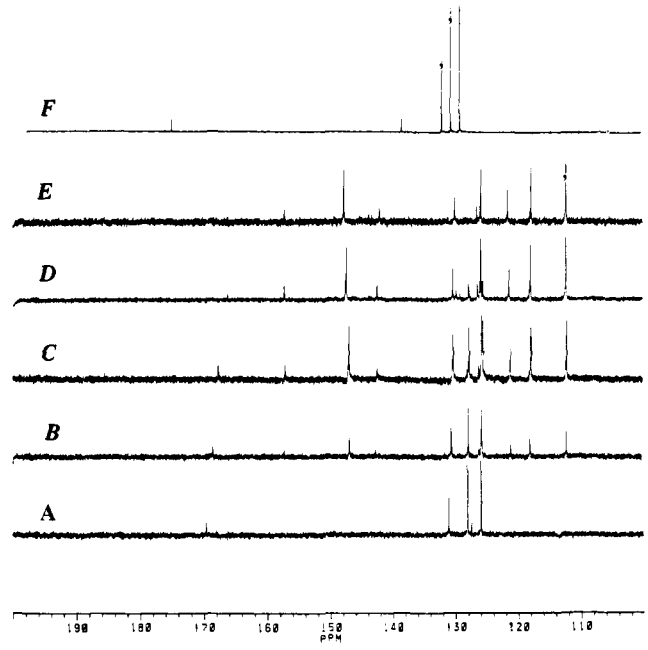

Figure 6. ^{13}C NMR resonances of varying concentrations of benzoic acid and *trans*-4-ethoxy-4′-stilbazole in CCl_4, except for F which was run in CD_3OD: (A) pure benzoic acid; (B) benzoic acid:stilbazole, 75:25 mol %; (C) benzoic acid:stilbazole, 50:50 mol %; (D) benzoic acid:stilbazole, 25:75 mol %; (E) pure *trans*-4-ethoxy-4′-stilbazole; (F) ammonium benzoate in CD_3OD.

hydrogen bond that this responsible for its rigidity, and despite this fact, the complex is highly thermally stable. The highest isotropization temperature, T_i, is observed for complex [**14b**/**16**] at 252 °C.

The DSC thermogram presented in Figure 5 (heating run) for complex [**13a**/**16**] annealed to 220 °C and then cooled to below its T_g is representative of the observations made for all complexes based on **16**. During the heating run, glass transition behavior is seen at 7 °C, while endothermic peaks which correspond to melting and isotropization are clearly observed at 126 and 229 °C, respectively. The broadness of the smectic to isotropic transition is likely due to the polydisperse nature of the polymers in these complexes. Heating to isotropization resulted in a slight darkening of the sample. On cooling, two exothermic peaks appeared at 228 and 88 °C. The reversibility of the peak near 228 °C during the heating–cooling cycle is indicative of a smectic to isotropic transition. The marked supercooling of the transition (126 °C during heating and 88 °C on cooling) during the cooling run is indicative of a smectic–solid phase transformation. A lower molecular weight sample of **12c** (M_w = 11 100, M_n = 6900) used in the preparation of [**12c**/**16**] was found to afford the same transition temperatures as its higher molecular weight analog reported in Table II.

X-ray diffraction studies indicate that all of the complexes of polysiloxanes **12–14** and stilbazole **16** shown in Table VII are predominantly crystalline below their respective K → S transitions. The coexistence of glassy and crystalline phases can be explained by the presence of both the highly ordered phase consisting of side-chain mesogenic complexes and the amorphous phase consisting of the dimethylsiloxane polymer backbone.[15] The identical transition temperatures (within experimental error) measured for blends [**12a**/**16**], [**13a**/**16**], and [**13b**/**16**] prepared from THF or pyridine solutions (Table VII) show that the solvent has no influence in the process of hydrogen-bond reorganization between the carboxy-ended polysiloxanes and stilbazole **16** during complex formation.

The frequencies of the OH stretch in the 1:1 blends of carboxy-ended polysiloxanes and stilbazole **16** are shown in Table IV. For these complexes, the OH stretch is split into three bands around 1900, 2550, and 2650 cm^{-1}, respectively. This pattern is indicative of a strong H-bonded system not involving proton

(29) (a) Vivas de Meftahi, M.; Frēchet, J. M. J. *Polymer* **1988**, *29*, 477. (b) Vivas de Meftahi, M. Ph.D. Thesis, University of Ottawa, Ontario, Canada, 1988.
(30) Nash, J. A.; Gray, G. W. *Mol. Cryst. Liq. Cryst.* **1974**, *25*, 299.
(31) Chiang, M.-C.; Hartung, W. H. *J. Org. Chem.* **1945**, *10*, 21.

Table VIII. X-ray Diffraction[a] Pattern of Blends of Some Carboxy-Ended Polysiloxanes and Stilbazole **16** (1 mol % COOH:1 mol % **16**)

blend	temp,[b] °C	layer spacing *d*, Å
[12a/16]	160	51.9 (s), 24.9 (w), 7.7 (d)
[12b/16]	160	57.6 (s), 28.7 (w), 8.0 (d)
	200	57.8 (s), 26.7 (w), 8.1 (d)
[12c/16]	160	61.5 (s), 31.2 (w), 7.9 (d)
[13a/16]	160	44.8 (s), 21.8 (w), 7.6 (d)
	200	47.2 (s), 22.4 (w), 7.6 (d)
	160[c]	44.8 (s), 22.4 (w), 7.8 (d)
	120[c]	56.0 (s), 28.0 (w), 7.8 (d)
[13b/16]	150	51.3 (s), 25.6 (w), 9.4 (d)
[13c/16]	150	54.6 (s), 28.1 (w), 8.6 (d)
	200	56.0 (s), 28.5 (w), 8.6 (d)

[a] A diffuse ring centered at 4.5 Å is found in all diffractions. s, strong diffraction; w, weak diffraction; d, diffuse. [b] All temperatures except where mentioned are reported for the heating run. [c] Temperature during cooling of the sample.

transfer.[18] Similar splitting patterns of the OH group are observed in polymer blends containing methacrylic acid and vinylpyridine groups.[32]

Further evidence for the exclusive involvement of H-bonding rather than proton transfer in the formation of the blends is provided by ^{13}C NMR model studies of mixtures of benzoic acid and *trans*-4-ethoxy-4′-stilbazole (**17**) in carbon tetrachloride. The ^{13}C NMR spectra of varying concentrations of benzoic acid and *trans*-4-ethoxy-4′-stilbazole are shown in Figure 6 (A–E), while Figure 6F shows the spectrum of ammonium benzoate in CD_3OD with its characteristic COO^- resonance at 175 ppm. The carbonyl carbon of benzoic acid, which resonates at 169.7 ppm (Figure 6A), is shifted upfield on addition of **17**, and the magnitude of the shift is proportional to the relative concentrations (Figure 6B–D). The carbonyl resonance moves upfield to 166.1 ppm for a COOH:**17** ratio of 1:3 (Figure 6D). The absence of a characteristic ^{13}C resonance for COO^- near 175 ppm indicates that proton transfer has not occurred. The liquid crystalline properties of complexes based on **17** will be described in the next section.

In order to confirm the molecular order and liquid crystallinity of the complexes, synchrotron X-ray diffraction measurements were performed on some unoriented equimolar complexes of carboxy-ended polysiloxanes and *trans*-4-[(4-methoxybenzoyl)-oxy]-4′-stilbazole (**16**) at various temperatures (Table VIII). The diffraction pattern for complex **[13a/16]** at 60 °C shows that it is crystalline, while at 160 °C the diffraction pattern indicates a smectic A or C state.[23-26] At room temperature, all of the complexes listed in Table VII are predominantly crystalline; however, crystallinity is more pronounced in complexes **[12a/16]** and **[13a/16]**.

Molecular modeling (Figure 7) combined with measured layer spacings (Table VIII) suggests that complexes **[12a/16]** → **[14b/16]** have either S_A or S_C phases, but optical microscopy reveals a *schlieren* texture that is typical of a smectic C phase.[33] Moreover, our preliminary work with complexes based on polysiloxanes **12,13** and optically active stilbazoles having the same mesogenic length shows that they exhibit spontaneous polarization, which confirms the presence of a chiral S_C phase in these materials. This also supports an S_C phase for equimolar complexes of carboxy-ended polysiloxanes and stilbazole **16**. Figure 8 outlines three possible arrangements for the S_C phase of **[13a/16]**. In the first (Figure 8A), the two H-bonded mesogenic units are placed end to end for an overall length of 68 Å, while in the second (Figure 8B) the two H-bonded mesogenic units have some lateral overlap for an overall length of less than 68 Å. The S_C structure shown in Figure 8B is likely preferred due to favorable dipole–dipole interactions between the overlapping mesogenic units in the smectic layer.

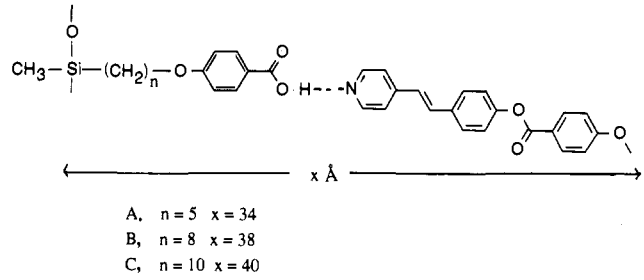

Figure 7. Molecular lengths for low molecular weight analogs of blends of polysiloxanes **12–14** and stilbazole **16**.

Cooling complex **[13a/16]** from 200 to 120 °C results in an increase of the layer spacing from 46.0 to 56.0 Å (Table VIII). This could be due to the reduction of tilt angle and/or variation of the repeat unit length with decreasing temperature. The tilt angle of low molecular weight mesogens invariably increases with decreasing temperature.[34] However, a decrease in tilt angle with decreasing temperature[35] has recently been reported for side-chain polysiloxanes. The repeat unit for complexes **[12a/16]**, **[12b/16]**, and **[12c/16]** increases linearly with the length of the alkyl chain (Table VIII). This confirms that the alkyl chains in the smectic layer are in an extended rather than a coiled conformation. Therefore, for a constant copolymer composition, the degree of lateral overlap between the H-bonded mesogens in complexes containing **16** is independent of the alkyl chain lengths in **12–14** (Scheme I).

The phase diagram for the binary blends of polysiloxane **13a** with varying amounts of **16** is shown in Figure 9. Polymer **13a** and stilbazole **16** are miscible over the entire range of composition. In contrast, phase separation and immiscibility are often observed[36] in the phase diagrams of binary mixtures of conventional liquid crystalline side chain polymers and low molecular weight liquid crystalline compounds. However, for our system, the existence of thermodynamically favorable hydrogen-bonding interactions is responsible for the miscibility between the polysiloxane and the stilbazole. The S → I transition curve shows a significant positive deviation, and the clearing temperatures are higher than those of either of the pure components because of the effect of the hydrogen bonding. Such remarkable deviations are not observed for the more common binary mixtures in which dipole–dipole interactions alone are the dominant factors. X-ray diffraction data were obtained for all of the blends of polysiloxane **12b** and **16**. These data indicate that all of the binary complexes (up to 88 mol % **12b**) are crystalline below their K → S transition temperature. However the amount of crystallinity is considerably reduced in blends containing more than 80 mol % **12b** (Figure 9). Optical microscopy[33] and X-ray diffraction study of the blends of **12b** and **16** indicate an S_C phase over a wide composition range (100 to 23 mol % **12b**). Complexes containing more than 80% of stilbazole **16** show a nematic phase, while complexes containing more than 20% of polymer exhibit a smectic phase.

Complexation of Side Chain (4-Alkoxybenzoic Acid) Terminated Polysiloxanes 12a–c to 14a–c with Nonmesogenic *trans*-4-Ethoxy-4′-stilbazole (17). In the preceding section, mesogenic *trans*-4-[(4-methoxybenzoyl)oxy]-4′-stilbazole (**16**) was used as a hydrogen-bond acceptor. However, *it is not necessary for both components to be liquid crystalline* for substantially the same observations to be made. This was demonstrated through the use of *trans*-4-ethoxy-4′-stilbazole (**17**) selected as a nonmesogenic H-bond acceptor significantly shorter in length along its long axis than stilbazole **16**. Therefore a shorter hydrogen-bonded mesogen can be expected to form through complexation with the various functional polysiloxanes. Stilbazole **17**, which only shows a K → I

(32) Lee, J. Y.; Painter, P. C.; Coleman, M. M. *Macromolecules* **1988**, *21*, 954.
(33) Demus, D.; Richter, L. *Textures of Liquid Crystals*; Deutscher Verlag: Leipzig, 1980.
(34) Gray, G. W.; Goodby, J. W. *Smectic Liquid Crystals*; Leonard Hill: Glasgow, 1984.
(35) Keller, E. N.; Nachaliel, E.; Davidov, D. *Phys. Rev. A* **1988**, *37*, 2251.
(36) Benthack-Thoms, H.; Finkelmann, H. *Makromol. Chem.* **1985**, *186*, 1895.
(37) Bruce, D. W.; Dunmur, D. A.; Lalinde, E.; Maitlis, P. M.; Styring, P. *Liq. Cryst.* **1988**, *3*, 385.

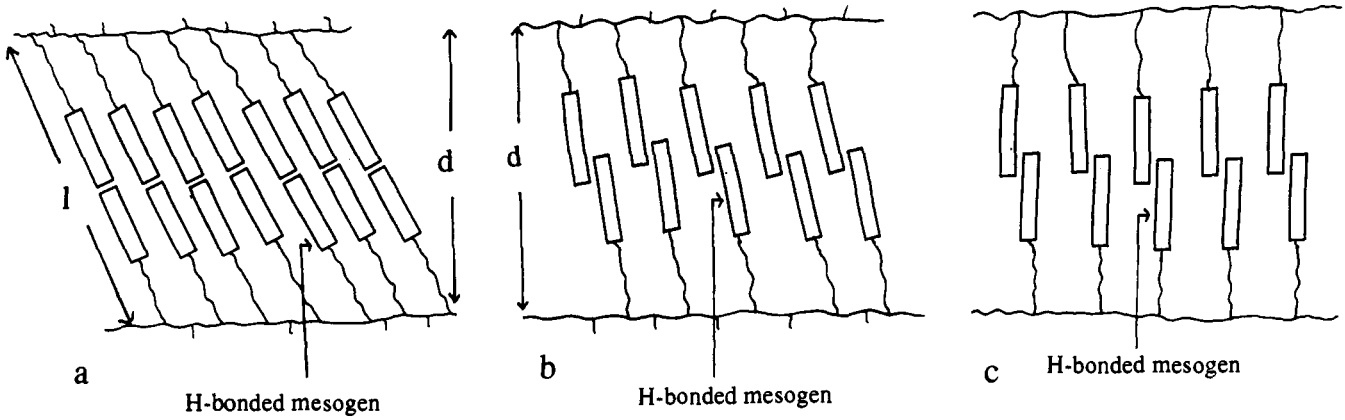

Figure 8. Schematic of the possible smectic C layers for blends of polysiloxanes **12a–c**, **13a–c**, and **14a,b** and stilbazole **16**. Data shown is for [**13a**/**16**] (d = layer spacing in Å): (A) repeat unit of the smectic layer made of two H-bonded mesogen units placed end to end; (B) repeat unit of the smectic layer made of two H-bonded mesogenic units placed sideways, resulting in some lateral overlap; (C) repeat unit of the S_A layer made of two laterally overlapping H-bonded mesogenic units.

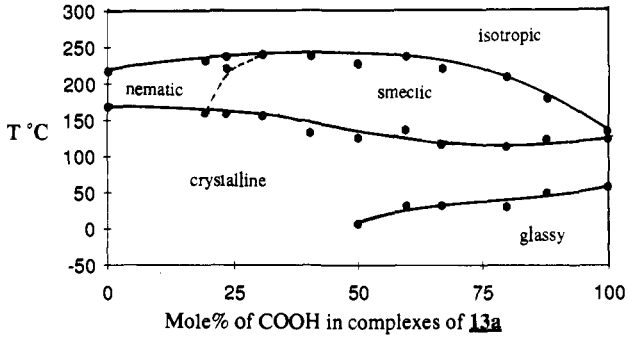

Figure 9. Phase diagram for binary blends of polysiloxane **13a** and stilbazole **16**.

Table IX. Phase Transition Temperatures[a] of 1:1 Complexes[b] of Polysiloxanes **12a–c**, **13a–c**, and **14a,b** and 4-Ethoxy-4′-stilbazole[c] (**17**) (Complexes Prepared from Pyridine Solution)

1:1 complex	$T_{K\rightarrow S}$, °C	$T_{S\rightarrow I}$, °C	ΔH_1,[d] J/g	ΔH_2,[e] J/g
[**12a**/**17**]	115	165	19.3	15.9
[**13a**/**17**]	114	182	21.6	15.2
[**14a**/**17**]	128	202	32.5	14.0
[**12b**/**17**]	100	174	18.2	13.8
[**13b**/**17**]	101	185	20.1	17.9
[**14b**/**17**]	112	212	29.4	15.9
[**12c**/**17**]	98	175	16.6	9.8
[**13c**/**17**]	98	178	17.1	8.0

[a] K → S, crystal to smectic transition; S → I, smectic to isotropic transition. [b] Equimolar amounts of the COOH group of the polysiloxanes and the stilbazole were used. [c] Crystalline material with melting point $T_{K\rightarrow I}$ 151 °C. [d] ΔH_1, enthalpy change for K → S transition in J/g of polymer blend. [e] ΔH_2, enthalpy change for S → I transition in J/g of polymer blend.

transition at 151 °C and no liquid crystalline state, was prepared as shown in Scheme III.

The thermal properties of the various complexes of **17** with polysiloxanes **12a–c**, **13a–c**, and **14a,b** are given in Table IX. Due to the lower isotropization temperatures of the complexes, samples which were heated to isotropization, T_I, and cooled to room temperature were used for DSC and polarized microscopy observation. The transition temperatures of the complexes based on **17** were not dependent on their thermal histories. Complexes based on **17** show lower clearing temperatures than those based on **16** due to the shorter length to diameter profile of the mesogen. For example, the isotropization temperature of complex [**12a**/**17**] is 62 °C lower than that of complex [**12a**/**16**]. Nevertheless, extended mesophases are clearly observed for all eight complexes including the complex between polymer **14a** and **17**, *for which neither of the pure components exhibits a mesophase.* DSC curves (both heating and cooling) were obtained for a once-annealed sample of the complex [**12a**/**17**] (representative of the behavior of all of the complexes based on **17**). During the heating run, melting and isotropization temperatures were clearly observed at 115 and 165 °C, respectively. No glass transition behavior was seen for any of the complexes. On cooling, two large exothermic peaks appeared at 164 and 101 °C, respectively. The near reversibility of the peak around 165 °C during the heating–cooling cycle indicates a smectic–isotropic transition. The supercooling of the transition (115 °C on heating and 101 °C on cooling) observed during the cooling run is indicative of a smectic–solid phase transformation.

Table X. X-ray Diffraction Pattern[a] of Equimolar Blends of Some Carboxy-Ended Polysiloxanes and Stilbazole **17** (1 mol % COOH:1 mol % **17**)

blend	temp,[b] °C	layer spacing d, Å
[**12a**/**17**]	155	49.8 (s), 24.2 (w), 8.0 (d)
	155[c]	49.8 (s), 24.2 (w), 8.0 (d)
[**12b**/**17**]	150	53.1 (s), 27.1 (w), 7.9 (d)
[**12c**/**17**]	150	55.5 (s), 27.4 (w), 7.9 (d)
[**13a**/**17**]	130	43.2 (s), 21.4 (w), 8.0 (d)
	160	42.1 (s), 20.8 (w), 8.1 (d)
	170	41.3 (s), 20.4 (w), 8.2 (d)
[**13b**/**17**]	150	48.0 (s), 23.3 (w), 9.2 (d)
[**13c**/**17**]	150	51.9 (s), 25.8 (w), 7.7 (d)
[**14b**/**17**]	160	37.4 (s), 19.5 (w), 12.9 (w), 9.7 (d)

[a] A diffuse ring centered at around 4.5 Å is seen in all diffraction patterns. s, m, and w are strong, medium, and weak reflections, respectively. [b] All temperatures except where mentioned are reported for the heating run. [c] Temperature during cooling run.

The IR frequencies of the OH stretch is some of the blends (1:1 ratio of COOH:**17**) of carboxy-ended polysiloxanes and *trans*-4-ethoxy-4′-stilbazole (**17**) are shown in Table IV. This pattern[18,32] of OH stretch is again indicative of strong H-bonding between the COOH of the polysiloxane and stilbazole **17**, with no proton transfer between the two components of the complex.

The OH stretch for the binary blends of **12a** and **17** containing from 80 to 37 mol % of the stilbazole is split into two bands centered around 1950 and 2500 cm^{-1} (1975 and 2520 cm^{-1} for the 1:1 complex). Upon decreasing the amount of stilbazole to 28 mol %, additional bands characteristic of self-association of **12a** to form a carboxylic acid dimer appear at 2970, 2645, and 2555 cm^{-1}, respectively. The OH stretch at 1930 cm^{-1} due to the H-bonding of the COOH group of polysiloxane to stilbazole **17** is seen even as the concentration of the latter is reduced to 18 mol %. This confirms that complexation of the carboxylic acid and the pyridine is thermodynamically favored over dimerization of the former.

X-ray diffraction data of some equimolar blends of carboxy-ended polysiloxanes and *trans*-4-ethoxy-4′-stilbazole are shown in Table X. Figure 10 shows flat plate diffraction photographs of [**12a**/**17**] at 80 and 155 °C; this confirms the crystallinity of

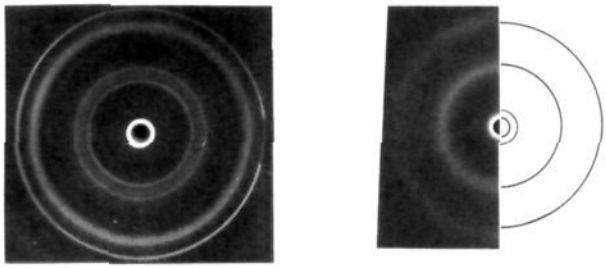

A B

Figure 10. X-ray diffraction of [**12a**/**17**] at various temperatures (heating run): (A) at 80 °C, showing crystallinity in the complex; (B) at 155 °C, showing the S_C phase.

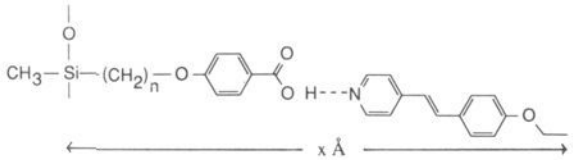

A, n = 5 x = 29
B, n = 8 x = 33
C, n = 10 x = 36

Figure 11. Molecular length for model mesogenic analogs of blends of polysiloxanes **12**–**14** and stilbazole **17**.

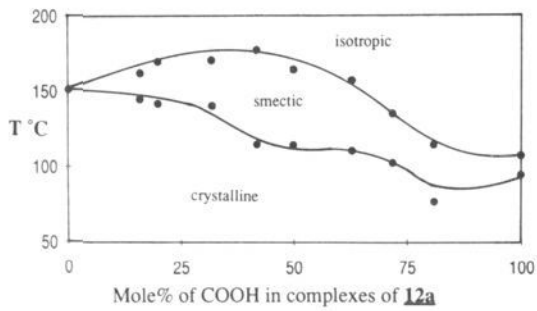

Figure 12. Phase diagram of binary blends between polysiloxane **12a** and stilbazole **17**.

the material below its K → S transition (Figure 10A). Molecular modeling (Figure 11) coupled with X-ray diffraction data (Table X) is indicative of either an S_A or S_C phase, with the repeat unit *made of two laterally overlapping H-bonded mesogenic units* (Figure 8B or C).

Figure 12 illustrates a phase diagram for the complex between **12a** and **17**. Extended mesophases are observed for the complexes formed using a wide range of H-bond donor to H-bond acceptor ratios. For example, a binary mixture containing only 20% of **12a** shows an extended smectic phase from 114 to 161 °C. X-ray diffraction for different binary complexes of **12a** and **17** also indicates either an S_C or S_A phase comprising laterally overlapping H-bonded mesogenic units (Figure 8B or C) over a wide range of compositions.

Conclusion

These results show that well-designed hydrogen-bonded systems can be used to build a novel type of side-chain liquid crystalline polymer and to induce liquid crystallinity in binary mixtures containing polymers. This may open a new avenue for the preparation of functional polymer liquid crystals, such as host–guest systems or ferroelectric coatings. This also constitutes a new type of molecular recognition in molecular aggregates since formation of these liquid crystalline complexes results from selective recognition between H-bonding donor polymers and H-bonding acceptor molecules. Current work in our laboratory builds on these findings to effect the self-assembly of hydrogen-bonded polymeric liquid crystalline complexes containing chiral groups for ferroelectric materials, dye molecules, strongly dipolar species, or mixed functionalities. These novel materials may prove useful in technological applications such as optical switching, display, or storage of information.

Experimental Section

Materials. *1-Bromo-4-pentene, 1-bromo-7-octene, 9-decen-1-ol, ethyl* 4-hydroxybenzoate, hydrogen hexachloroplatinate, benzyl bromide, 4-picoline, 4-hydroxybenzaldehyde, cyclohexene, 10% Pd/C, and cesium carbonate were purchased from Aldrich Chemical Co. Poly(methylhydrosiloxanes) and poly(methylhydrosiloxane-*co*-dimethylsiloxanes) were obtained from Petrarch (catalog nos. PS120, PS123, PS122.5). All of the above were used without further purification except for 1-bromo-4-pentene and cyclohexene, which were distilled before use. Toluene and isopropyl alcohol were dried by boiling overnight over sodium and calcium hydride, respectively, and then distilled. Hydrogen hexachloroplatinate was handled in a dry box.

Characterization. Infrared (IR) spectra were recorded on a Nicolet IR/44 FTIR spectrometer. All IR spectra except those used for monitoring the hydrosilylation reaction were recorded with KBr pellets. KBr was dried at 150 °C overnight under vacuum. NMR spectra were measured on an IBM-Bruker AF300 spectrometer. The ^{13}C NMR spectra of mixtures of benzoic acid and *trans*-4-ethoxy-4′-stilbazole in CCl_4 shown in Figure 6A–E were run in a 10-mm tube at a benzoic acid concentration of 2.0 mg/mL of CCl_4. To maximize sensitivity, 30 000 scans were collected for each experiment. Differential scanning calorimetry (DSC) transitions were recorded on a Mettler DSC 30 low-temperature cell. DSC transitions of carboxy-ended polysiloxanes **12a**–**c**, **13a**–**c**, **14a**, and their blends with *trans*-4-ethoxy-4′-stilbazole (**17**) were recorded after heating the sample to isotropization and then cooling to −40 °C (15–20 °C/min). DSC transitions of blends of polysiloxanes **12a**–**c**, **13a**–**c** and **14a**,**b** and *trans*-4-[(4-methoxybenzoyl)oxy]-4′-stilbazole (**16**) shown in Tables VII and VIII were recorded after heating the sample to 200 or 220 °C and then cooling below its T_g, as heating above T_i resulted in sample decomposition. Gel permeation chromatography (GPC) was done on a Nicolet LC/9560 liquid chromatograph equipped with three 5-μm PL gel columns, a Milton Roy refractometer, and a differential viscometer (Viscotek Corp., Model 110). Both the refractometer and the viscometer were calibrated against narrow molecular weight polystyrene standards using THF as eluent, and universal calibration software (Viscotek Corp.) was used to process the data. The flow rate was 1 mL/min. Optical microscopy was done using an Olympus BH-2 microscope equipped with a Mettler FP-82 hot stage and crossed polarizers. The textures were observed after annealing the sample for several hours at a given temperature. X-ray studies were done in the Wilson Synchrotron Laboratory at Cornell University using sample holders made of 25 × 25 mm aluminum plates 2 mm in thickness with a 2-mm hole (sample compartment) in the center. The sample was mounted onto a Mettler FP-82 hot stage aligned with the collimated (0.5 mm) 1.54-Å X-ray beam. The diffraction patterns were recorded on a flat film (Kodak DEF-5) placed at a distance of 90–110 mm from the sample. Bragg's equation was used to calculate the layer or *d* spacings of the various reflections.

Synthesis of 1-Bromo-9-decene (1c). To 15.6 g (99.8 mmol) of 9-decen-1-ol in 40 mL of dry THF under N_2 was added 34.7 g (105 mmol) of carbon tetrabromide, followed by the slow addition of 26.7 g (102 mmol) of triphenylphosphine. During the course of the addition of triphenylphosphine, the contents of the flask warmed up to 60 °C. Stirring was continued for 1 h after the addition of triphenylphosphine was completed. The progress of the reaction was monitored by TLC using hexane/ethyl acetate (10:1) as solvent. After removal of THF and extraction of the 1-bromo-9-decene formed from the reaction mixture using a 10:1 mixture of hexane/ethyl acetate, purification was performed by flash silica gel column chromatography using hexane/ethyl acetate (10:1) as eluent. After drying in vacuo for 24 h, the desired product was obtained in 91% yield: ^1H NMR ($CDCl_3$, ppm) 5.81 (CH═), 5.00 (CH_2═), 3.45 ($BrCH_2$), 2.08 (═CHCH_2), 1.88 ($BrCH_2CH_2$), 1.50–1.20 (aliphatics).

Synthesis of 4-(ω-Alkenyloxy)benzoic Acids 4a–c. A general procedure for the preparation of (ω-alkenyloxy)benzoic acids is given below. Ethyl 4-hydroxybenzoate 10.0 g (60.2 mmol) was alkylated with 58.7 mmol of ω-alkenyl bromide and 4.0 g (58.7 mmol) of sodium ethoxide in boiling ethanol. Workup and purification with flash silica gel chromatography using dichloromethane/hexane (2:1) as eluent gave ethyl 4-(ω-alkenyloxy)benzoates **3a**–**c** as a colorless oil. Hydrolysis of the ethyl 4-(ω-alkenyloxy)benzoates **3a**–**c** was achieved by boiling in aqueous ethanolic KOH for 3–8 h, depending on the length of the alkyl chain in **3**. After acidification with 5% HCl solution, the precipitate was washed and dried under vacuum.

Ethyl 4-(ω-Alkenyloxy)benzoates 3a–c. ^1H NMR for **3a** ($CDCl_3$, ppm): 8.01, 6.92 (aromatic), 5.85 (CH═CH_2), 5.00 (CH═CH_2), 4.37

($COOCH_2$), 4.02 (OCH_2), 2.07 (CH_2=$CHCH_2$), 1.80 ($COOCH_2CH_2$), 1.20–1.50 (aliphatic). Anal. Calcd for **3b** ($C_{17}H_{24}O_3$): C, 73.92; H, 8.70. Found: C, 74.00; H, 8.67. Anal. Calcd for **3c** ($C_{19}H_{28}O_3$): C, 75.00; H, 9.21. Found: C, 74.78; H, 9.16.

4-(ω-Alkenyloxy)benzoic Acids 4a–c. Yields based on ethyl 4-hydroxybenzoate: 4-(4-pentenyloxy)benzoic acid (**4a**) 88%; 4-(7-octenyloxy)benzoic acid (**4b**) 84%; 4-(9-decenyloxy)benzoic acid (**4c**) 64%. ^{1}H NMR for **4a** ($CDCl_3$, ppm): 8.05, 6.90 (aromatic), 5.85 (=CH), 5.04 (CH_2=), 3.95 (OCH_2), 2.73 (=$CHCH_2$), 1.91 (OCH_2CH_2), 1.30–1.50 (aliphatic). IR: 1680 cm^{-1} (C=O). Anal. Calcd for **4a** ($C_{12}H_{14}O_3$): C, 69.88; H, 6.84. Found: C, 69.79; H, 6.77. Anal. Calcd for **4b** ($C_{15}H_{20}O_3$): C, 72.55; H, 8.12. Found: C, 72.49; H, 8.03. Anal. Calcd for **4c** ($C_{17}H_{24}O_3$): C, 73.88; H, 8.75. Found: C, 73.84; H, 8.60. The transition temperatures for the three acids **4a–c** were as reported previously in the literature.[38]

Synthesis of Benzyl 4-(ω-Alkenyloxy)benzoates 5a–c. The desired 4-(ω-alkenyloxy)benzoic acid prepared above (30.1 mmol) was dissolved in 80 mL of DMF under N_2 atmosphere at room temperature, and 7.05 g (21.6 mmol) of Cs_2CO_3 was added. After 10 min of stirring at room temperature, 5.3 g (31 mmol) of benzyl bromide was added. The resulting mixture was stirred for 20 h at room temperature. After the removal of solvent, the product was extracted with $CHCl_3$. The organic layer was washed with aqueous saturated $NaHCO_3$ and then water and dried over anhydrous $MgSO_4$. Remaining traces of acid were removed by passing the product through a short silica gel column using CH_2Cl_2/hexane (3:1) as eluent. Yield: benzyl 4-(4-pentenyloxy)-benzoate (**5a**) 90%; benzyl 4-(7-octenyloxy)benzoate (**5b**) 84%; benzyl 4-(9-decenyloxy)benzoate (**5c**) 86%. ^{1}H NMR ($CDCl_3$, ppm): 8.03, 6.92, 7.40 (aromatic), 6.82 (CH=), 5.35 ($C_6H_5CH_2$), 4.87 (CH_2=), 4.02 (OCH_2), 2.08 (=$CHCH_2$), 1.81 (OCH_2CH_2), 1.25–1.50 (aliphatic). IR: 1727 cm^{-1} (C=O). Anal. Calcd for $C_{19}H_{20}O_3$: C, 77.03; H, 6.76. Found: C, 76.82; H, 6.96. Anal. Calcd for $C_{22}H_{26}O_3$: C, 78.11; H, 7.70. Found: C, 78.48; H, 8.09. Anal. Calcd for $C_{24}H_{30}O_3$: C, 78.69; H, 8.20. Found: C, 78.65; H, 8.18.

Synthesis of Polysiloxanes 9a–c, 10a–c, and 11a,b. A generalized procedure for the hydrosilylation reaction is given: Poly(methylhydrosiloxane) **8** or poly(methylhydrosiloxane-*co*-dimethylsiloxanes) **6,7** (10.0 mmol of SiH groups) and 11.0 mmol of benzyl 4-(ω-alkenyloxy)benzoate **5** were added to 30 mL of dry toluene under N_2 atmosphere. To this solution was added from 0.40 to 0.0060 mmol (depending on substrate) of H_2PtCl_6 in dry isopropyl alcohol. The resulting mixture was stirred for 12–18 h at 80 °C. The reaction was monitored by observing the disappearance of the SiH stretching at 2160 cm^{-1} in the IR spectrum. IR spectra of the reaction mixture were run on sodium chloride discs. After cooling, the reaction mixture was concentrated, and the excess of alkene **5a–c** was separated from the polysiloxanes **9a–c**, **10a–c**, or **11a,b** by passing the reaction mixture through a flash silica gel column using dichloromethane/hexane (2:1) as eluent. The polysiloxanes **9a–c**, **10a–c**, or **11a,b** were then eluted from the column using tetrahydrofuran (THF). A highly viscous liquid was obtained after removal of THF. No remaining alkene **5a–c** could be seen by TLC, NMR, and IR spectroscopy. The yield of polysiloxanes **11a,b** (85–88%) was lower than that for polysiloxanes **9a–c** or **10a–c** (90–95%) because it is more difficult to elute the homopolymer completely during its chromatographic purification. ^{1}H NMR analysis confirmed that hydrosilylation was quantitative due to the disappearance of the SiH peak at 4.8 ppm. ^{1}H NMR ($CDCl_3$, ppm): 8.00, 7.35, 6.85 (aromatic), 5.30 ($C_6H_5CH_2$), 3.90 (OCH_2), 1.72, 1.35, 0.45 (aliphatic), 0.05 ($Si(CH_3)O$). IR: 1727 cm^{-1} (C=O).

Preparation of Polysiloxanes 12a–c, 13a–c, and 14a,b. The following is a typical procedure for the removal of benzyl protecting groups from polysiloxanes **9a–c**, **10a–c**, or **11a,b**. A solution of 1.00 g of polysiloxane **10a** in a mixture of 25 mL of THF and 5 mL of EtOH containing 0.10–0.30 g of 10% Pd/C was degassed for 1 h. Then 10–15 equiv of distilled cyclohexene per equivalent of benzyl ester group was added, and the mixture was boiled for 4 days under N_2 atmosphere. After cooling, the reaction mixture was filtered through Celite, and the filtrate was concentrated and precipitated into hexane. The resulting white solid was washed with hexane and dried under vacuum at 60 °C for 15 h. Yield, 85–90%. The molecular weights of the polysiloxanes **12a–c**, **13a–c**, and **14a,b** are given in Table II. ^{1}H NMR (DMSO-d_6 at 67 °C, ppm): 7.96, 6.97 (aromatic), 4.02 (OCH_2), 3.15 (COOH), 1.00–1.75 (aliphatic), 0.01 ($Si(CH_3)O$). ^{13}C NMR for a representative polysiloxane **14a** in (DMSO-d_6 at 67 °C, ppm): 166.5 (COO), 162.0, 131.5, 123.5, 114.0 (C_6H_4), 67.5 (OCH_2), 29.0, 28.0, 22.5, 17.0 (CH_2) 0.0 (OCH_3). IR: 1674 cm^{-1} (C=O).

Synthesis of *trans*-4-Hydroxy-4′-stilbazole. The following is a modification of the procedure of Chiang and Hartung.[31] *trans*-4-Hydroxy-4′-stilbazole was made by an aldol reaction of 4-hydroxybenzaldehyde (21.0 g, 0.172 mol) and 4-methylpyridine (16.0 g, 0.172 mol) in acetic anhydride (40 mL) at 120 °C. Hydrolysis of *trans*-4-acetoxy-4′-stilbazole with aqueous alcoholic sodium bicarbonate solution gave *trans*-4-hydroxy-4′-stilbazole as a pale yellow solid. ^{1}H NMR for *trans*-4-acetoxy-4′-stilbazole ($CDCl_3$, ppm): 8.55, 7.35 (pyridyl), 7.53, 7.12 (phenyl), 7.29, 6.95 (CH=CH), 2.30 ($OOCCH_3$). *trans*-4-Hydroxy-4′-stilbazole yield based on 4-hydroxybenzaldehyde, 37%. ^{1}H NMR (acetone-d_6, ppm): 8.50, 7.45 (pyridyl), 7.53, 6.90 (phenyl), 7.45, 7.08 (CH=CH).

Synthesis of *trans*-4-[(4-Methoxybenzoyl)oxy]-4′-stilbazole (16). *trans*-4-Hydroxy-4′-stilbazole (3.53 g, 17.9 mmol) was dissolved in 80 mL of pyridine under nitrogen atmosphere. The solution was cooled to 0 °C, and 0.10 g (0.82 mmol) of (*N*,*N*-dimethylamino)pyridine was added. A solution of *p*-methoxybenzoyl chloride (3.16 g, 18.5 mmol) in THF (10 mL) was added dropwise over a period of 30 min, and the mixture was allowed to warm up to room temperature. After stirring for 5 h at room temperature and for 10 h at 60 °C, the mixture was cooled and the solvent was evaporated. The resulting solid was treated with 100 mL of water. The precipitate was filtered and then washed with water. The product was purified on a flash silica gel column using chloroform/methanol (30:1) as eluent followed by recrystallization from acetone to afford 5.9 g (91%) of the desired product. The transition temperatures of **16**, K → N at 168 °C and N → I at 216 °C were in accordance with our earlier preparation.[10] Nash and Gray have reported a nematic range of 140–230 °C for the same compound.[30] ^{1}H NMR ($CDCl_3$, ppm): 8.60, 7.37 (pyridyl), 7.61, 7.23 (OC_6H_4CH=), 8.17, 7.00 (OC_6H_4COO), 3.90 (OCH_3). Anal. Calcd for $C_{21}H_{17}NO_3$: C, 76.11; H, 5.17; N, 4.22. Found: C, 75.97; H, 5.15; N, 4.11.

Synthesis of *trans*-4-Ethoxy-4′-stilbazole (17). *trans*-4-Hydroxy-4′-stilbazole (1.45 g, 7.35 mmol) was dissolved in 25 mL of DMF under N_2 atmosphere, followed by addition of 2.09 g (14.7 mmol) of K_2CO_3 and 0.80 g (7.3 mmol) of ethyl bromide. After the reaction was stirred at room temperature for 24 h, DMF was removed and the product extracted with $CHCl_3$. The $CHCl_3$ layer was washed with 5% aqueous NaOH and then repeatedly with water to neutral pH. Purification was done by flash silica gel column chromatography using dichloromethane/methanol (30:1) as eluent to give 1.65 g (80%) of the desired product. **17** was further purified by recrystallization from aqueous acetone, mp 151 °C (lit.[37] mp 153.5 °C). ^{1}H NMR ($CDCl_3$, ppm): 8.53, 7.32 (pyridyl), 7.45, 6.90 (phenyl), 7.25, 6.85 (CH=CH), 4.05 (OCH_2), 1.45 (CH_3).

Preparation of Complexes of 12a–c, 13a–c, and 14a,b with 16 and 17. The requisite amounts of **12a–c**, **13a–c**, or **14a,b** and **16** or **17** were dissolved in dry pyridine, and the solvent was removed by slow evaporation. The blend was then dried at 60–70 °C in vacuo.

Acknowledgment. Financial support of this research by an unrestricted gift from IBM Corporation (Materials and Processing Science Program), the Cornell University Material Science Center (NSF DMR-8818558), and S. C. Johnson and Sons is gratefully acknowledged. In addition, special thanks are due to Mr. P. G. Wilson for technical assistance and to the operating staff of the Cornell High Energy Synchrotron Laboratory for their valuable assistance during X-ray diffraction studies.

Supplementary Material Available: Tables of phase transition temperatures, layer spacings, and OH stretching frequencies (Tables 11–14) and a figure displaying the X-ray diffraction of **[13a/16]** (Figure 13) (5 pages). Ordering information is given on any current masthead page.

(38) Kelly, S. M.; Buchecker, R. *Helv. Chim. Acta* **1988**, *71*, 461.